

Supporting Information: DNA Damage Emanating From a Neutral Purine Radical Reveals the Sequence Dependent Convergence of the Direct and Indirect Effects of γ -Radiolysis

Liwei Zheng and Marc M. Greenberg*

Department of Chemistry
Johns Hopkins University
3400 N. Charles St.
Baltimore, MD 2128

mgreenberg@jhu.edu

Contents:

1. **Experimental procedures.** (S3-S7)
2. **Table S1.** UPLC gradient table. (S5)
3. **Figure S1.** Autoradiogram of aerobic photolysis of 5'-³²P-**2**. (S8)
4. **Figure S2.** Autoradiogram of aerobic photolysis of 5'-³²P-**2**. (S9)
5. **Figure S3.** Autoradiogram of aerobic photolysis of 3'-³²P-**2**. (S10)
6. **Figure S4.** Autoradiogram of anaerobic photolysis of 5'-³²P-**2**. (S11)
7. **Figure S5.** Autoradiogram of aerobic photolysis of 5'-³²P-**3**. (S12)
8. **Figure S6.** Autoradiogram of aerobic photolysis of 5'-³²P-**4**. (S13)
9. **Figure S7.** Autoradiogram of aerobic photolysis of 5'-³²P-**5**. (S14)
10. **Figure S8.** Autoradiogram of aerobic photolysis of 5'-³²P-**6**. (S15)
11. **Figure S9.** Autoradiogram of aerobic photolysis of 5'-³²P-**7**. (S16)
12. **Figure S10.** Autoradiogram of aerobic photolysis of 5'-³²P-**8**. (S17)
13. **Figure S11.** Autoradiogram of aerobic photolysis of 5'-³²P-**9**. (S18)
14. **Figure S12.** Autoradiogram of aerobic photolysis of 5'-³²P-**10**. (S19)
15. **Figure S13.** Autoradiogram of aerobic photolysis of 5'-³²P-**11**. (S20)
16. **Figure S14.** Autoradiogram of aerobic photolysis of 3'-³²P-**11**. (S22)
17. **Figure S15.** Sequence and pH influence on strand damage following piperidine treatment. (S23)
18. **Figure S16.** pH Effect on strand damage in duplex **6**. (S23)
19. **Figure S17.** pH Effect on strand damage in duplex **7**. (S24)
20. **Figure S18.** pH Effect on strand damage in duplex **11**. (S24)
21. **Figure S19.** Representative chromatogram for determination of conversion of **1** in DNA by UPLC. (S25)
22. **Table S2.** Estimated efficiency of hole transfer (pH = 5.1) (S26)
23. **Figure S20.** UPLC-MS of the strand of **2** containing **1**. (S27)
24. **Figure S21.** ESI-MS of the strand of **3** containing **1**. (S27)
25. **Figure S22.** UPLC-MS of the strand of **4** containing **1**. (S28)
26. **Figure S23.** UPLC-MS of the strand of **5** containing **1**. (S28)
27. **Figure S24.** ESI-MS of the strand of **6** containing **1**. (S29)
28. **Figure S25.** ESI-MS of the strand of **7** containing **1**. (S29)
29. **Figure S26.** ESI-MS of the strand of **8** containing **1**. (S30)
30. **Figure S27.** ESI-MS of the strand of **9** containing **1**. (S30)
31. **Figure S28.** ESI-MS of the strand of **10** containing **1**. (S31)
32. **Figure S29.** ESI-MS of the strand of **11** containing **1**. (S31)

- 33. ^1H NMR and ^{13}C NMR of **S1**. (S32)
- 34. ^1H NMR and ^{31}P NMR of **S2**. (S33)

General methods. All solvents were distilled before use. Dichloromethane, DIPEA and pyridine were distilled from CaH_2 . Oligonucleotides were synthesized on an Applied Biosystems Incorporated 394 oligonucleotide synthesizer. Oligonucleotide synthesis reagents were purchased from Glen Research (Sterling, VA). T4 polynucleotide kinase, and terminal transferase were obtained from New England Biolabs and γ - ^{32}P -ATP and α - ^{32}P -cordycepin 5'-triphosphate were purchased from Perkin Elmer. C18-Sep-Pak cartridges were obtained from Waters and Poly-Prep columns from Bio-Rad. All photolyses were carried out in Pyrex using a Rayonet photoreactor fitted with 16 lamps having a maximum output at 350 nm. PBS buffer (0.1 M NaCl, 10 mM sodium phosphate, pH 7.2 and pH 6.0), sodium citrate buffer (0.1 M NaCl, 10 mM sodium citrate, pH 5.1) and water were treated by Chelex® 100 resin. All anaerobic photolyses were carried out in sealed Pyrex tubes, which were degassed by freeze-pump-thaw degassing (3 cycles). Samples were sealed while under vacuum at 77 K. Photolyses of DNA were carried out for 8 h. Quantification of radiolabeled oligonucleotides was carried out using a Molecular Dynamics Phosphorimager 860 equipped with ImageQuant Version TL software. ESI-MS was carried out on a Thermoquest LCQDeca. UPLC-MS analysis was carried out on Waters Acquity/Xevo-G2 UPLC-MS system equipped with ACQUITY UPLC HSS T3 Column (100Å, 1.8 μm , 2.1 mm X 100 mm). UPLC analysis was carried out on Agilent 1290 infinity UPLC equipped with ACQUITY UPLC HSS T3 Column (100Å, 1.8 μm , 2.1 mm X 100 mm).

Oligonucleotide synthesis. Commercially available fast deprotecting phosphoramidites

were used for DNA synthesis of oligonucleotides containing **1**. A 5 min coupling time was used for the modified phosphoramidite (**S2**). Deprotection of synthesized oligonucleotides containing **1** was performed with concentrated ammonia for 16 h at room temperature, followed by concentration under reduced pressure. The dried products were purified using 20% denaturing PAGE.

Typical sample preparation for photolysis. The strand (1 μ M) containing the radical precursor was labeled at the 5' end with γ -³²P-ATP using T4 PNK in T4 PNK buffer (70 mM Tris-HCl, pH 7.6, 10 mM MgCl₂, 5 mM DTT, 45 min, 37 °C). For experiments using duplex DNA, the labeled strand was hybridized to the complementary strand (1.5 eq.) in PBS (0.1 M NaCl, 10 mM sodium phosphate pH 7.2) by heating at 90°C for 1 min and slowly cooling to room temperature. The hybridized duplexes were diluted to 0.1 μ M in buffer before subjecting to photolysis.

Post-photolysis treatments. Aliquots from photolyzed solutions or unphotolyzed controls were treated with piperidine (1 M, 30 min, 90 °C), Fpg (1.25 μ M, 1 μ L, 10 mM Bis Tris-Propane HCl (pH 7), 10 mM MgCl₂, 1 mM DTT, 100 μ g/mL BSA, 1 h, 37 °C), or Ir⁴⁺ (0.1 mM of Na₂IrCl₆•6H₂O) for 1 h at 25 °C, quenched (2 mM Hepes, 10 mM EDTA, pH 7), and treated with piperidine (1 M, 30 min, 90 °C). Alternatively, photolysates were treated with piperidine (1 M, 30 min, 90 °C) in the presence of 0.25 M BME. All samples treated with enzymes were precipitated (0.3 M NaOAc, pH 5.2, 0.1 g/mL CT DNA) with ethanol.

Piperidine treated samples were evaporated to dryness under vacuum, and washed 2x with 10 μ L water, which was also removed under vacuum. Samples were analyzed by dissolving in formamide loading buffer prior to running in 20% denaturing PAGE. BME, piperidine, and Ir⁴⁺ solutions were always prepared fresh on the day of the experiment.

Enzymatic digestion of oligonucleotides to 2'-deoxynucleosides for UPLC analysis.

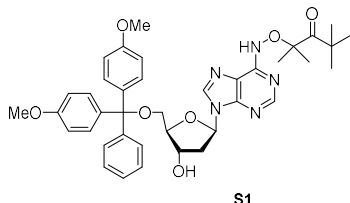
The unphotolyzed duplexes and the corresponding photolysates (4 pmol) in 1.6 μ L H₂O, 10 \times DNA degradase plus® buffer (5 μ L) and dU (2.5 μ L, 80 μ M) as internal standard were incubated with DNA degradase plus® (2 μ L, 5 U/ μ L) for 4 h at 37 °C. The reaction mixture was filtered through nanosep® 3K filter by centrifuging the mixture for 5-10 min at 16000 \times g. The filter was washed once with 25 μ L H₂O and the combined filtrate (50 μ L) was then analyzed using an Agilent 1290 infinity UPLC. The gradient is shown in Table S1.

Table S1

Time/min	Flow/ mL	%A	%B
0	0.3	95.0	5.0
2	0.3	95.0	5.0
9.5	0.3	20.0	80.0
12.0	0.3	20.0	80.0
13.0	0.3	95.0	5.0
16.0	0.3	95.0	5.0

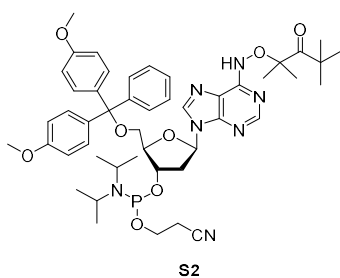
A: 10 mM ammonium formate and B: acetonitrile.

Preparation of phosphoramidite precursor (S1). Radical precursor¹ (104 mg, 0.26 mmol), was



azeotropically dried with pyridine three times. Pyridine (2 mL) and DMTCI (106 mg, 0.32 mmol) were added. The reaction was stirred at room temperature overnight. The reaction was concentrated under vacuum, and purified by flash chromatography (50% ethyl

acetate in DCM) on a silica column to give **S1** as a light yellow foam (96 mg, 53%). ¹H NMR (400 MHz, MeOH-d₄) δ 7.87 (s, 1H), 7.55 (s, 1H), 7.38 – 7.31 (m, 2H), 7.30 – 7.20 (m, 4H), 7.16 (t, *J* = 7.4 Hz, 2H), 7.12 – 7.07 (m, 1H), 6.74 (dd, *J* = 8.9, 1.4 Hz, 4H), 6.29 (t, *J* = 6.3 Hz, 1H), 4.56 (dd, *J* = 9.4, 4.0 Hz, 1H), 4.10 (q, *J* = 4.3 Hz, 1H), 3.32 – 3.28 (m, 2H), 2.83 – 2.70 (m, 1H), 2.43 (ddd, *J* = 13.5, 6.4, 4.3 Hz, 1H), 1.47 (s, 6H), 1.22 (s, 9H). ¹³C NMR (101 MHz, MeOH-d₄) δ 160.0, 146.3, 145.4, 142.1, 137.9, 137.2, 137.0, 131.3, 131.2, 129.3, 128.7, 127.8, 120.4, 114.0, 88.6, 88.0, 87.5, 85.9, 72.7, 65.1, 61.5, 55.7, 45.2, 40.9, 29.3, 25.2, 20.9, 14.5. IR (neat) 3273 (broad), 2932, 1691, 1659, 1592, 1463, 1301, 1250, 1176, 1035, 954, 887, 829, 754, 700, 660 cm⁻¹. HRMS (ESI-TOF) *m/z* calcd for (C₃₉H₄₆N₅O₇)⁺ (*M* + *H*)⁺ = 696.3397, found *m/z* = 696.3392.



Preparation of phosphoramidite S2. DIPEA (66.3 mg, 89.3 μL, 0.54 mmol), DCM (3.5 mL) was added to **S1** (96 mg, 0.14 mmol). The reaction was stirred at 0 °C, and 2-cyanoethyl N,N-diisopropylchlorophosphoramidite (40.5 mg, 0.17 mmol) was

added dropwise. The reaction was concentrated under vacuum, and purified by flash chromatography (50% ethyl acetate in hexane) on a silica column to give **S2** as white foam (74 mg, 59%). ¹H NMR (400 MHz, MeOH-d₄) δ 7.88 (d, *J* = 2.1 Hz, 1H), 7.53 (d, *J* = 2.1 Hz, 1H), 7.44

– 7.33 (m, 2H), 7.31 – 7.23 (m, 4H), 7.23 – 7.06 (m, 3H), 6.88 – 6.62 (m, 5H), 6.29 (td, $J = 6.4$, 3.1 Hz, 1H), 4.85 (s, 1H), 4.83 – 4.73 (m, 1H), 4.29 – 4.14 (m, 1H), 3.88 – 3.52 (m, 12H), 3.42 – 3.35 (m, 1H), 3.02 – 2.83 (m, 1H), 2.69 – 2.40 (m, 4H), 1.47 (s, 6H), 1.23 (s, 9H), 1.15 (m, 14H). ^{31}P NMR (162 MHz, MeOH- d_4) δ 148.39, 148.26. HRMS (ESI-TOF) m/z calcd for $(\text{C}_{48}\text{H}_{63}\text{N}_7\text{O}_8\text{P})^+$ ($\text{M} + \text{H}$) $^+ = 896.4476$, found $m/z = 896.4471$.

Reference

(1) Zheng, L.; Griesser, M.; Pratt, D. A.; Greenberg, M. M. *J. Org. Chem.* **2017**, *82*, 3571.

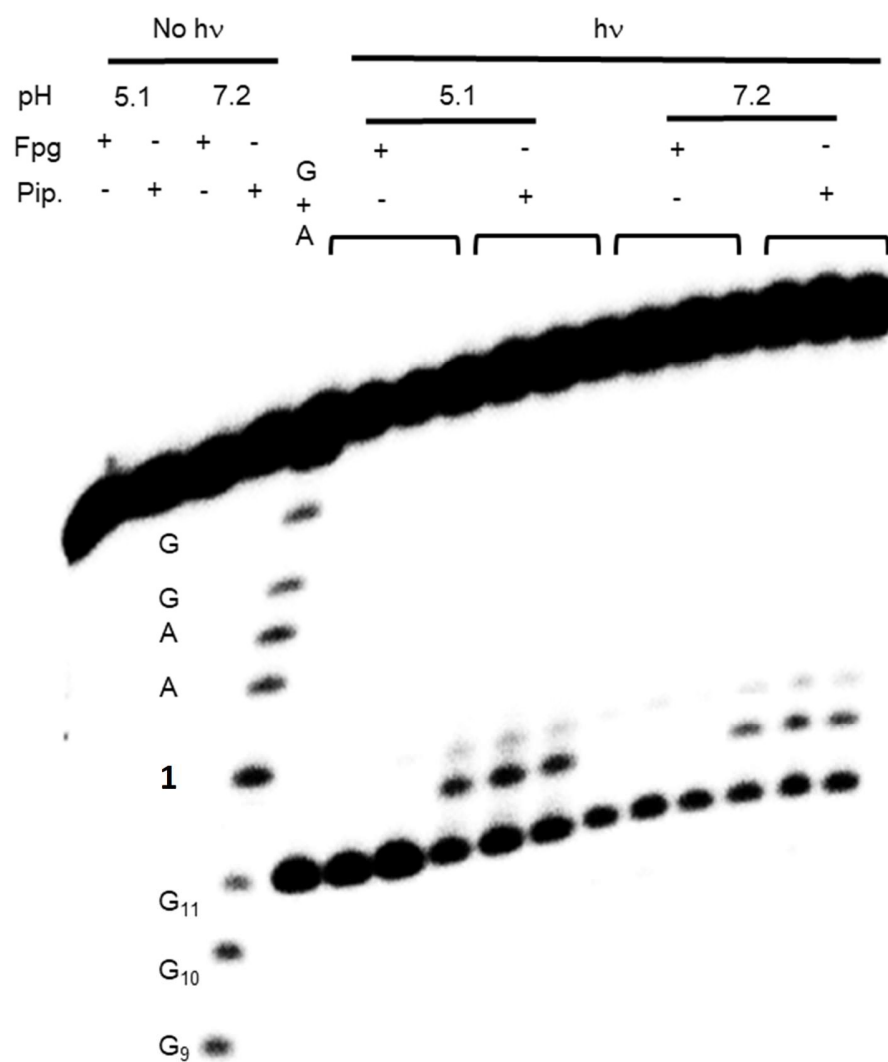


Figure S1. Autoradiogram of aerobic photolysis of 5'-³²P-**2**, followed by chemical and enzymatic treatments.

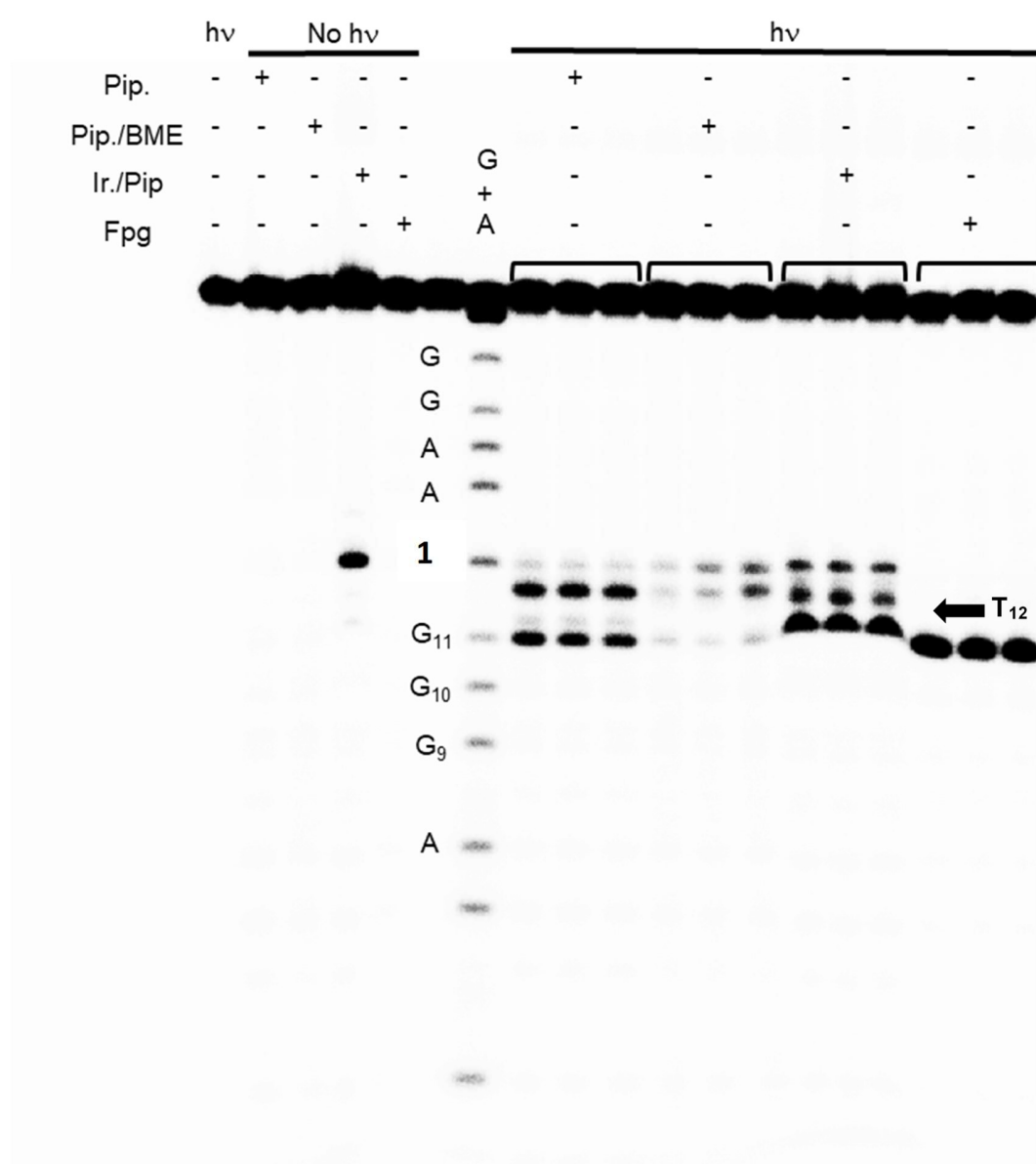


Figure S2. Autoradiogram of aerobic photolysis of 5'-³²P-**2**, followed by chemical and enzymatic treatments.

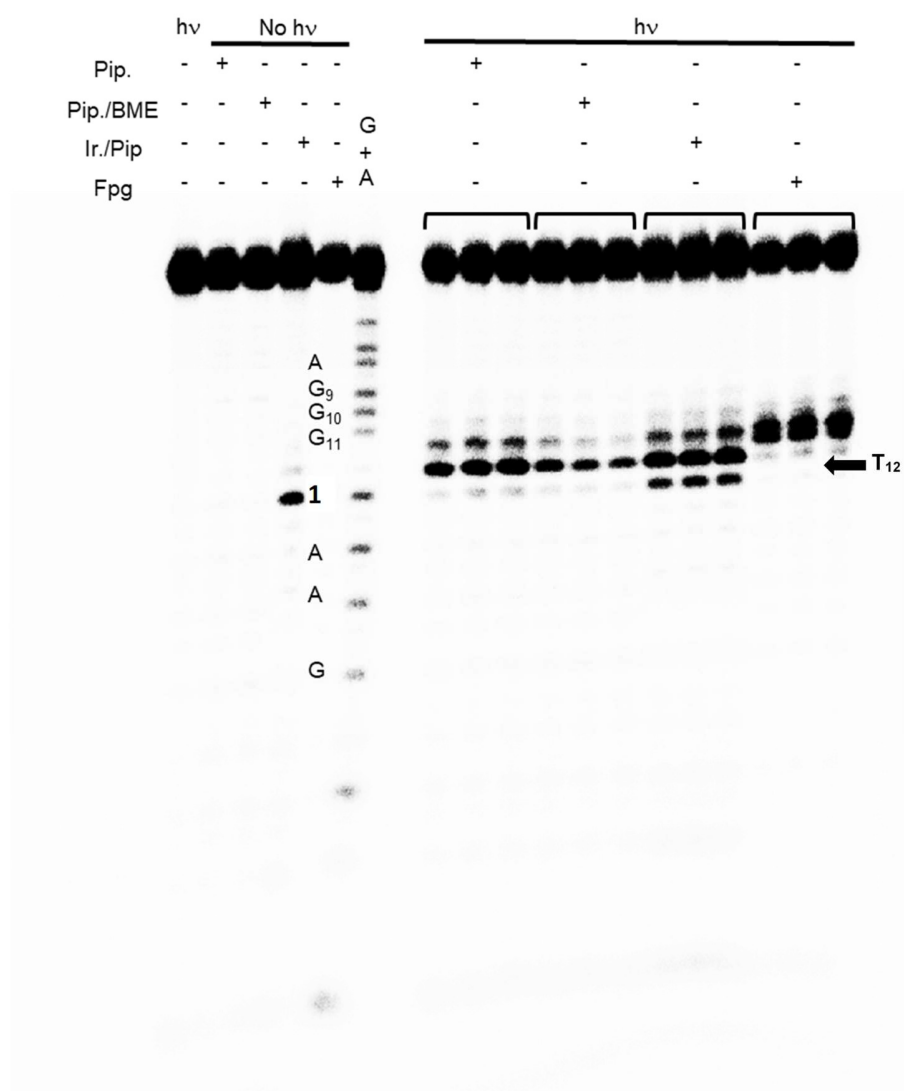


Figure S3. Autoradiogram of aerobic photolysis of 3'-³²P-**2**, followed by chemical and enzymatic treatments.

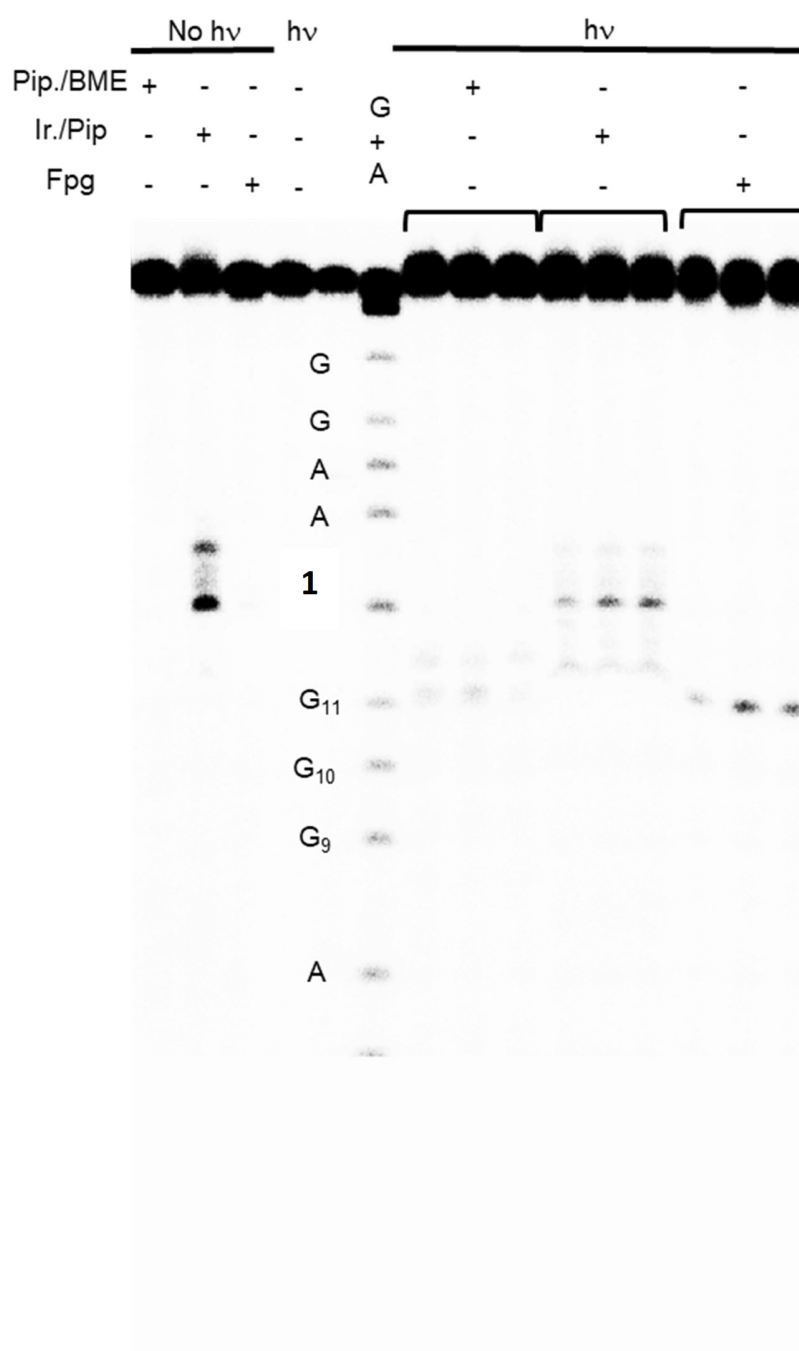


Figure S4. Autoradiogram of anaerobic photolysis of 5'-³²P-2, followed by chemical and enzymatic treatments.

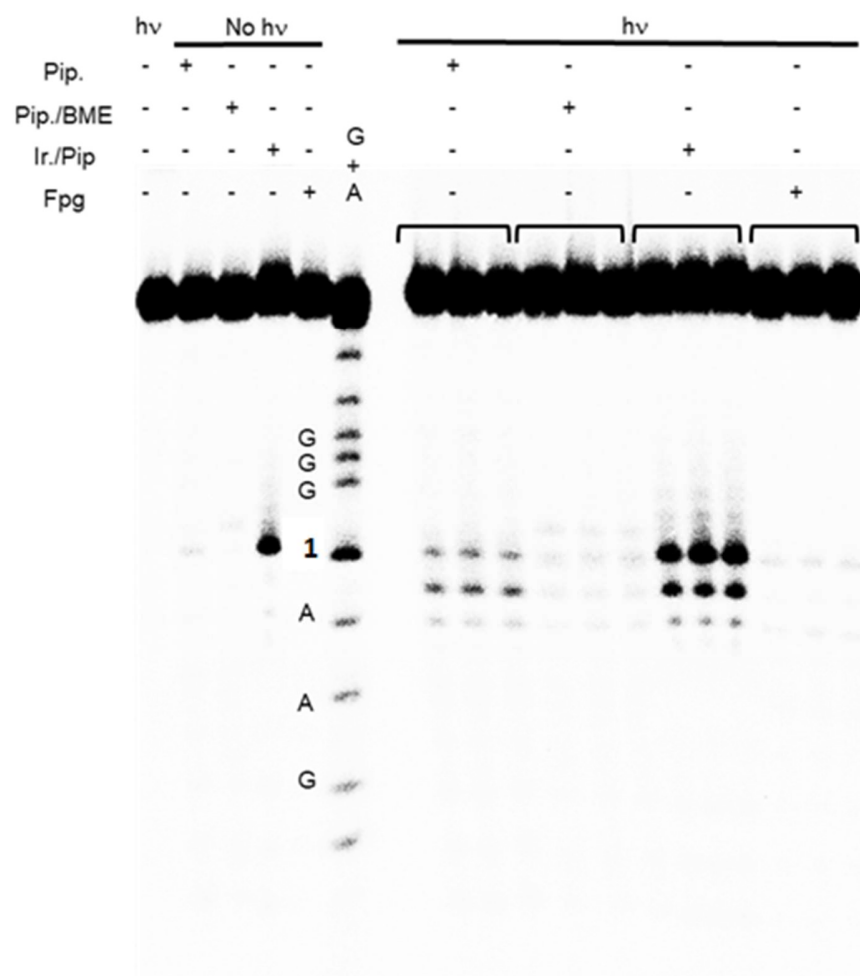


Figure S5. Autoradiogram of aerobic photolysis of 5'-³²P-**3**, followed by chemical and enzymatic treatments.

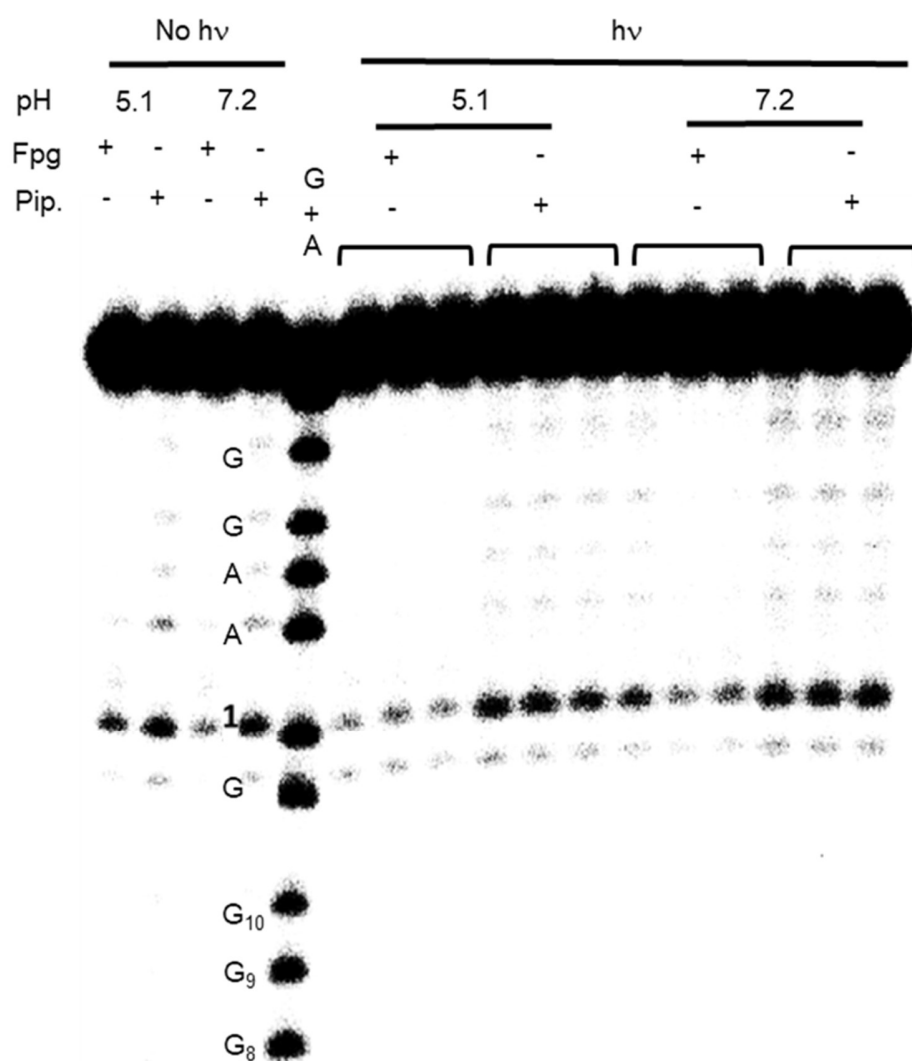


Figure S6. Autoradiogram of aerobic photolysis of 5'-³²P-**4**, followed by chemical and enzymatic treatments.

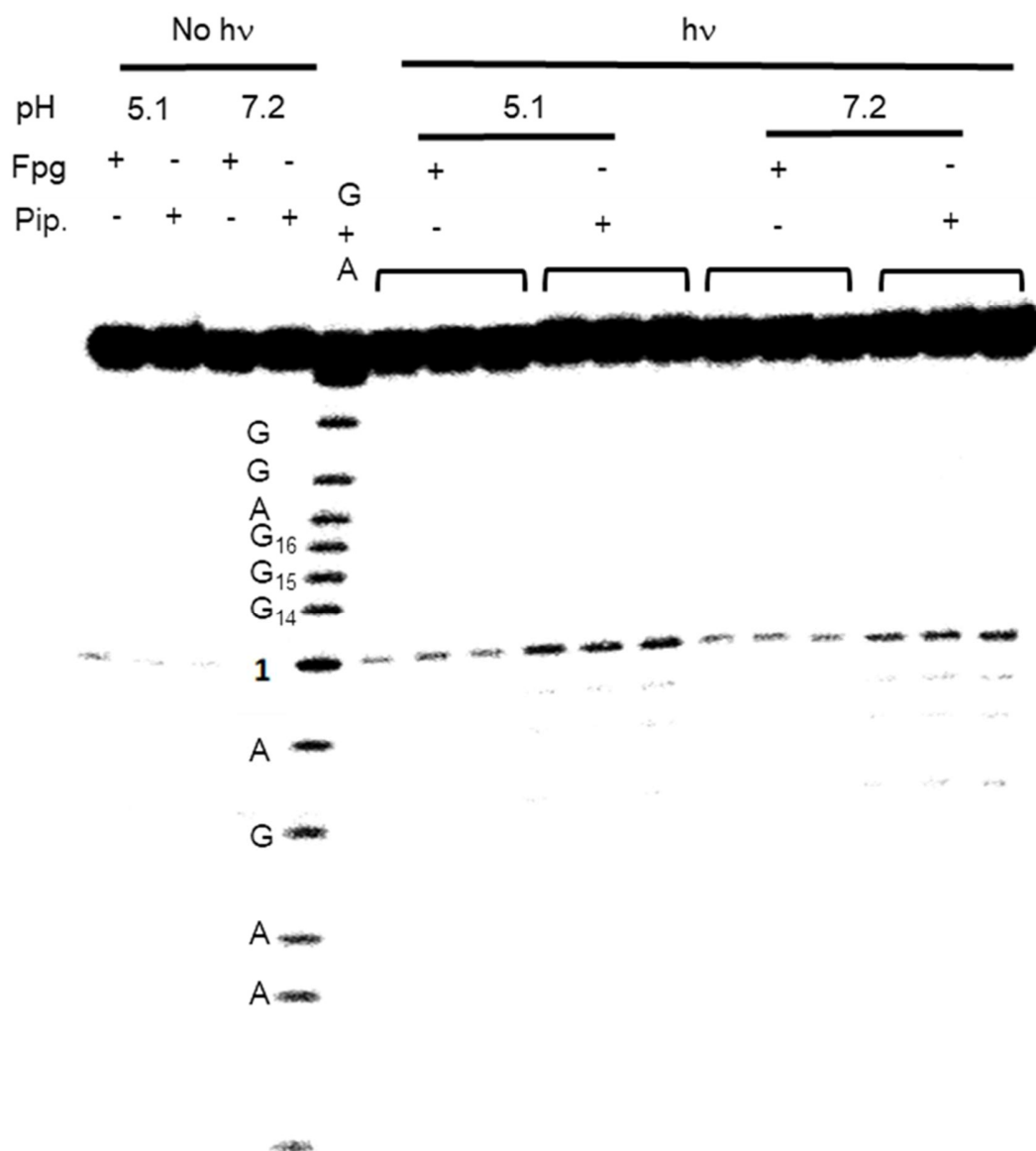


Figure S7. Autoradiogram of aerobic photolysis of 5'-³²P-5, followed by chemical and enzymatic treatments.

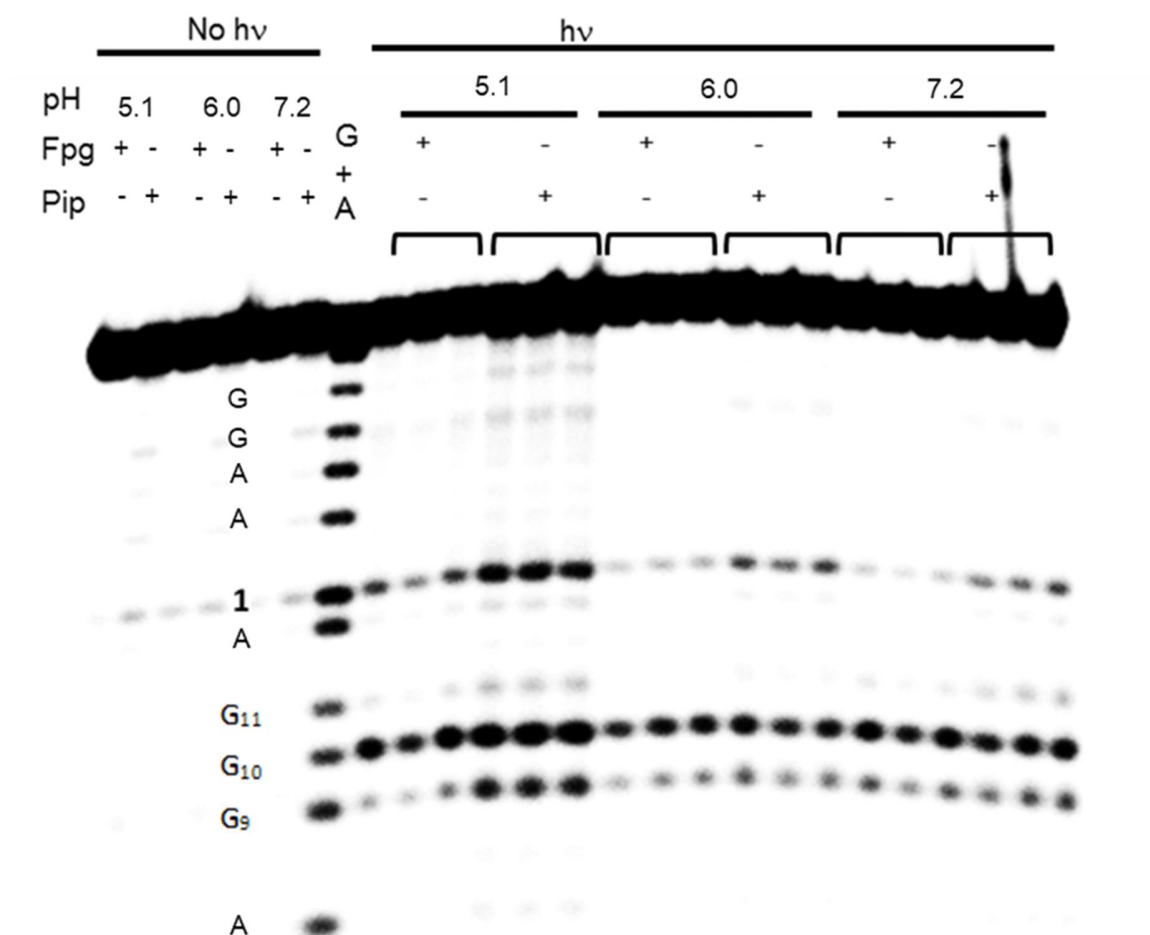


Figure S8. Autoradiogram of aerobic photolysis of 5'-³²P-**6**, followed by chemical and enzymatic treatments.

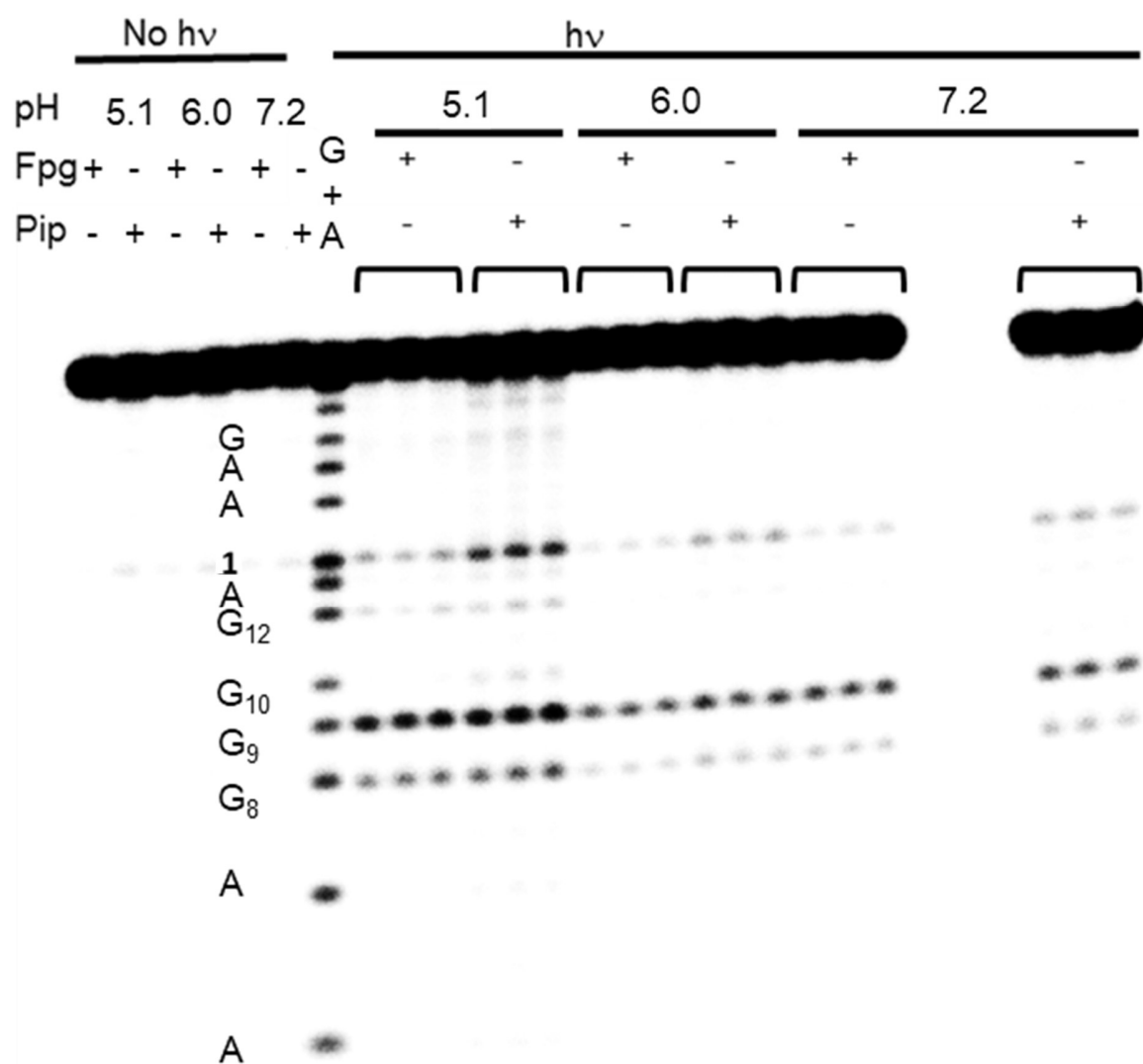


Figure S9. Autoradiogram of aerobic photolysis of 5'-³²P-7, followed by chemical and enzymatic treatments.

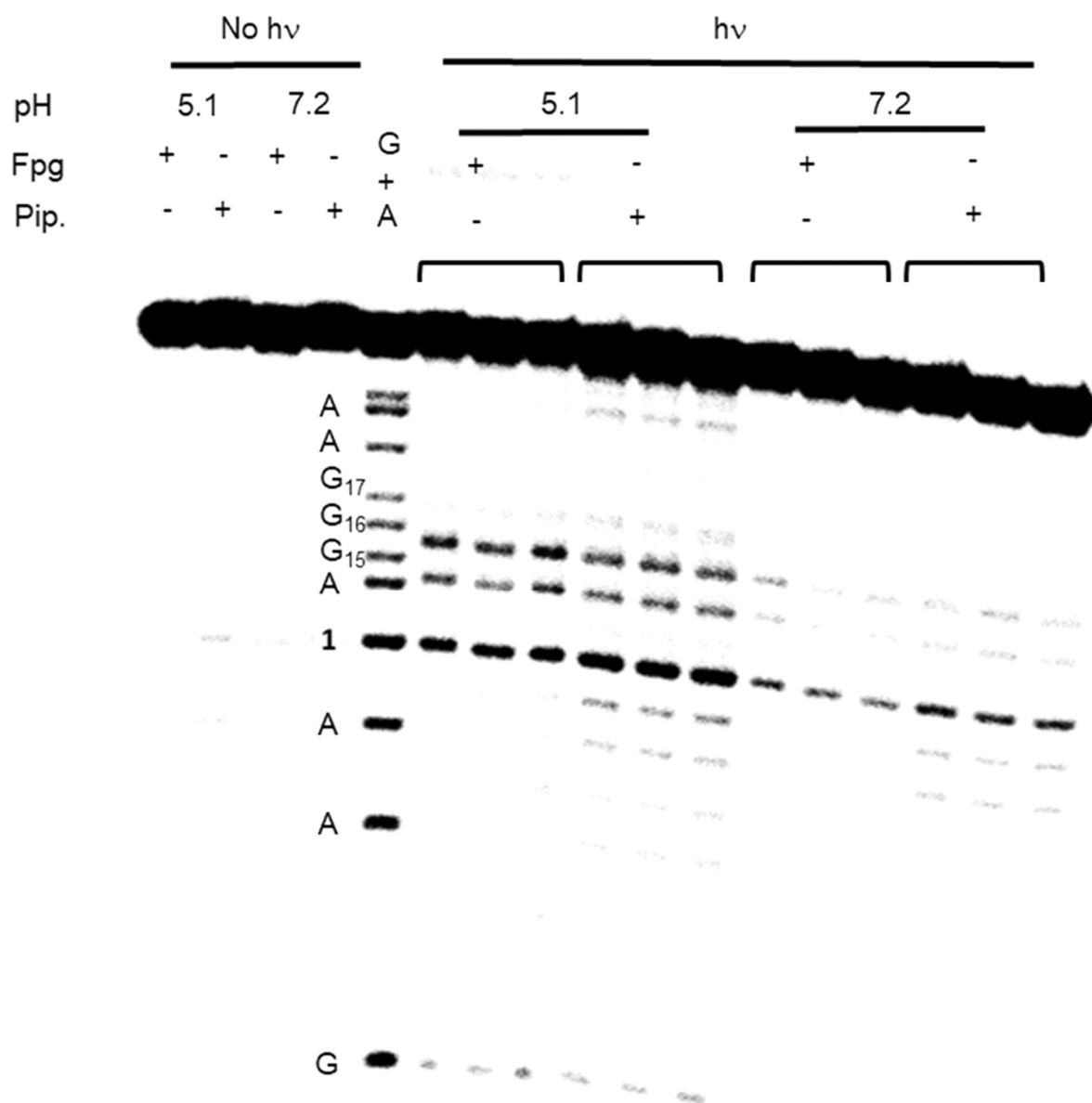


Figure S10. Autoradiogram of aerobic photolysis of 5'-³²P-8, followed by chemical and enzymatic treatments.

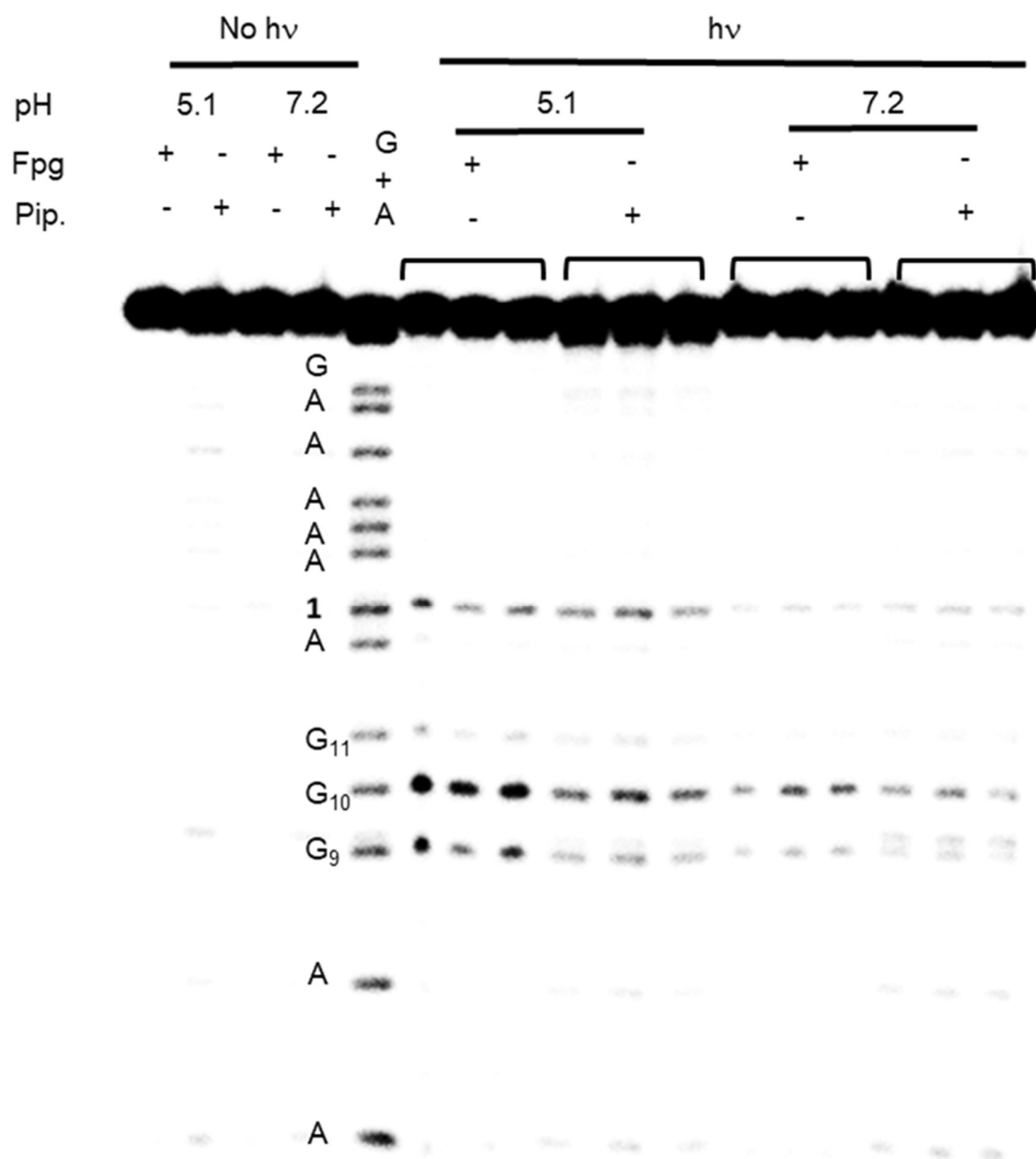


Figure S11. Autoradiogram of aerobic photolysis of 5'-³²P-9, followed by chemical and enzymatic treatments.

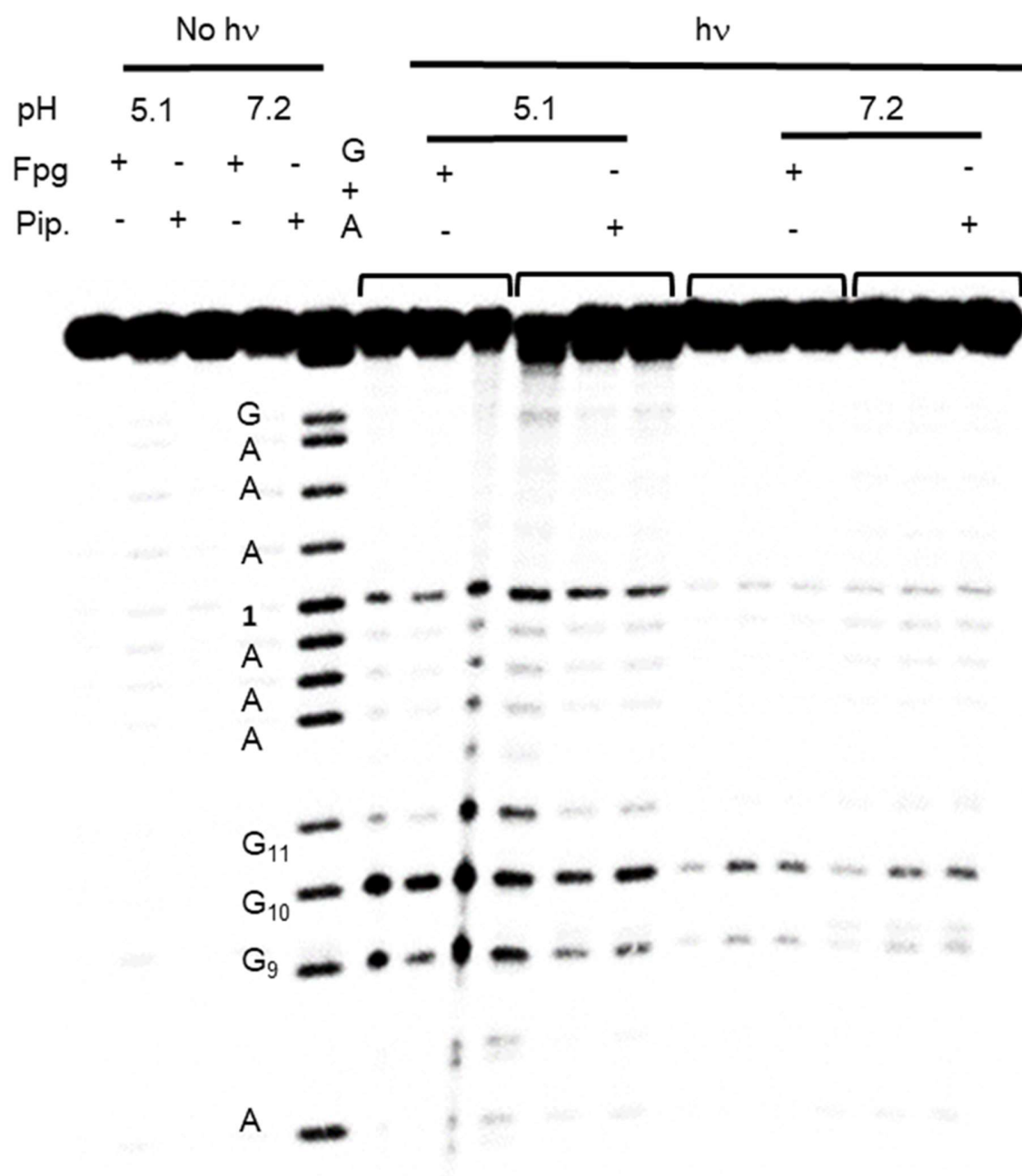
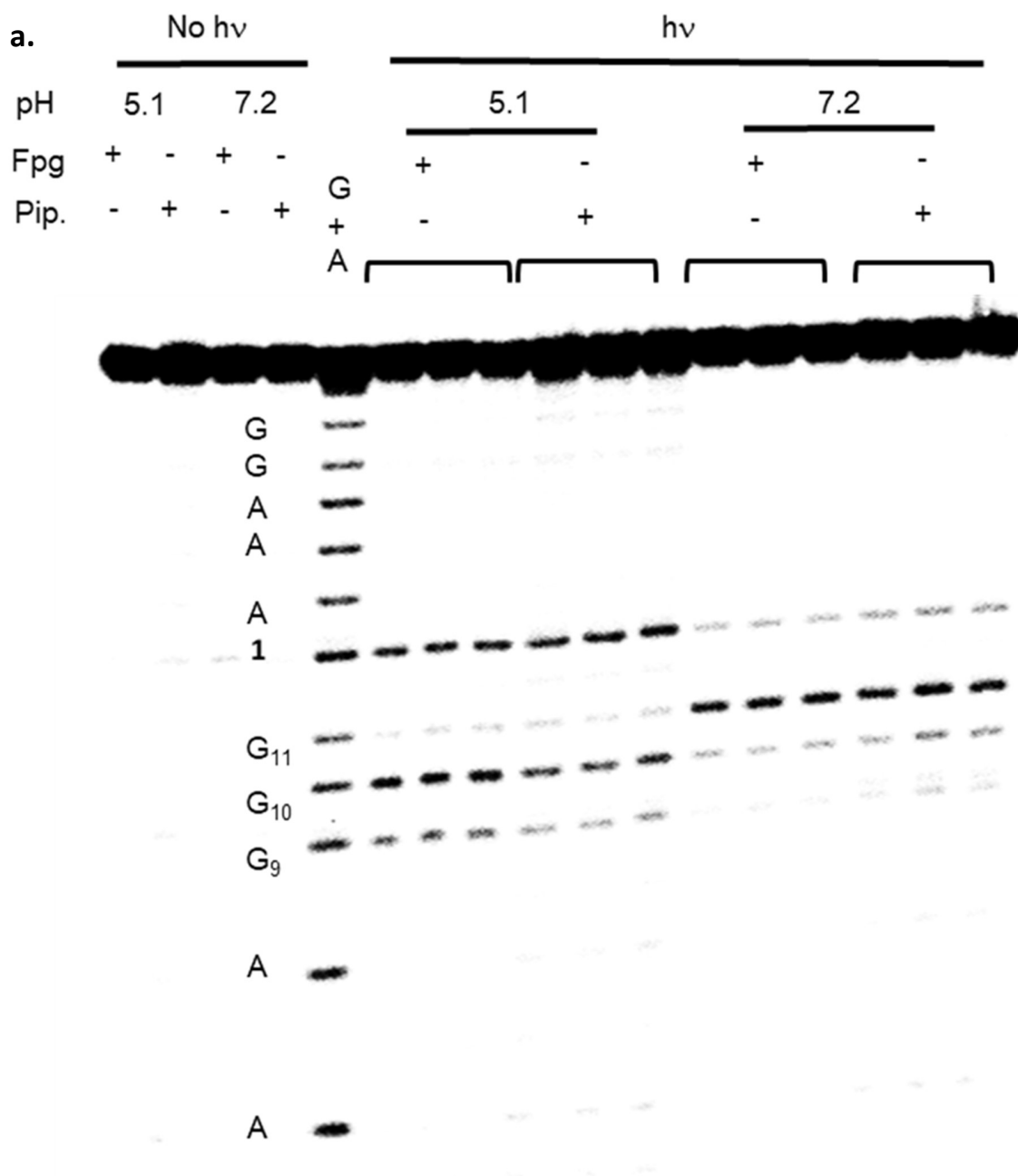


Figure S12. Autoradiogram of aerobic photolysis of 5'-³²P-10, followed by chemical and enzymatic treatments.



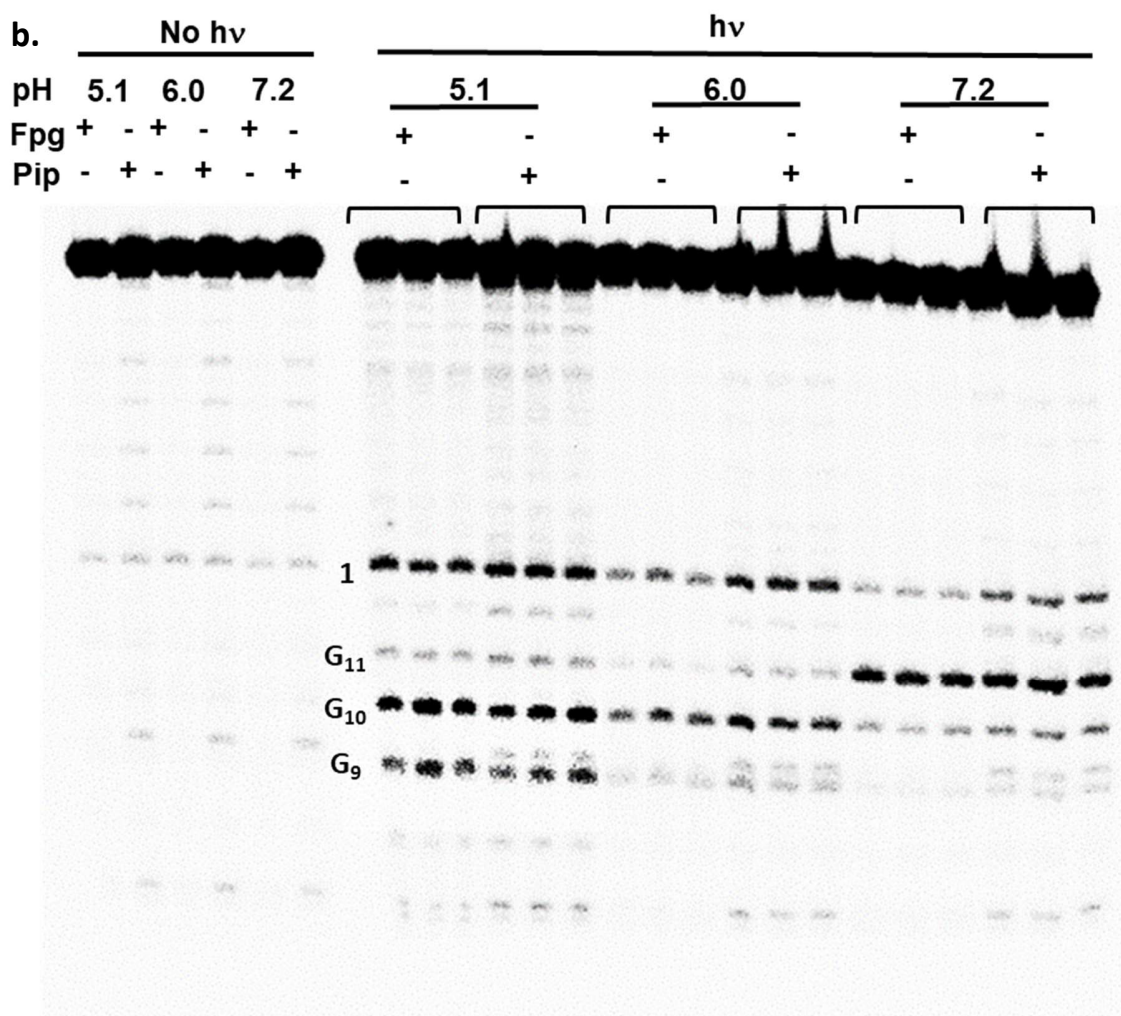


Figure S13. Autoradiogram of aerobic photolysis of 5'-³²P-11, followed by chemical and enzymatic treatments: (a) pH 5.1 and 7.2, (b) pH 5.1, 6.0 and 7.2.

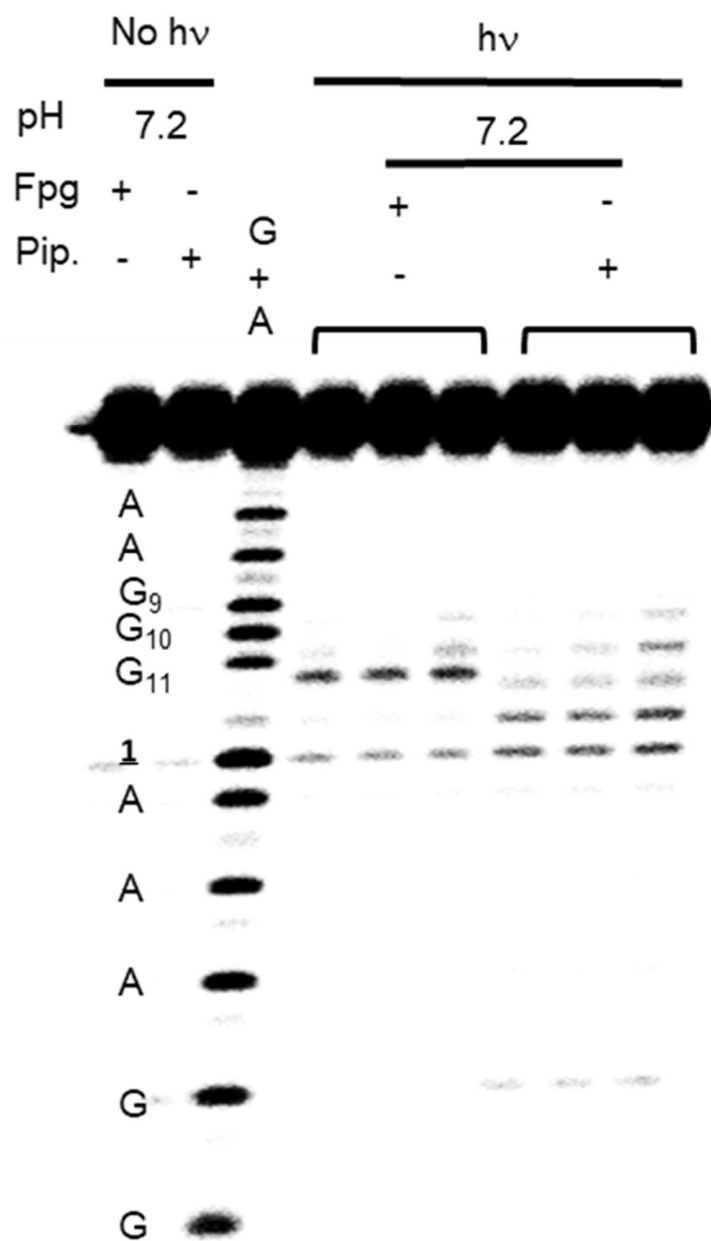


Figure S14. Autoradiogram of aerobic photolysis of 3'-³²P-11, followed by chemical and enzymatic treatments.

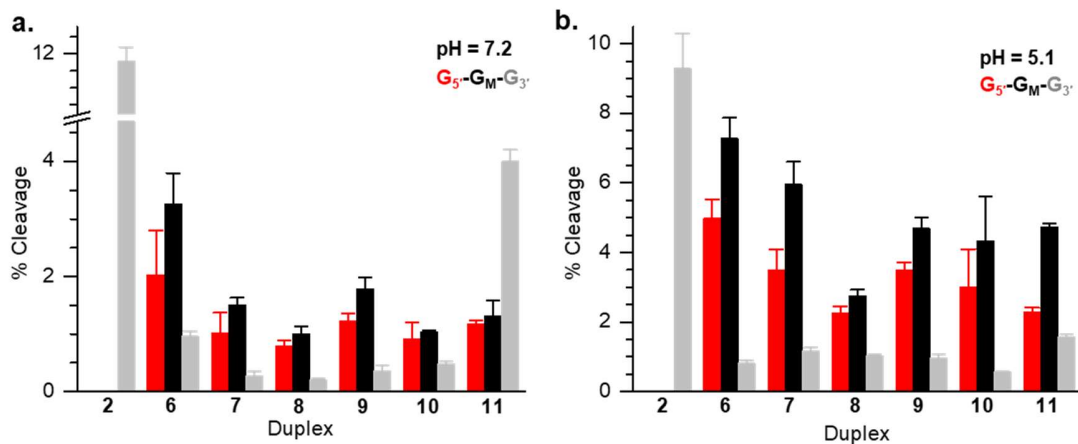


Figure S15. Sequence and pH influence on strand damage following piperidine treatment. (a) pH 7.2 (b) pH 5.1. G_5' , G_M' , and $G_{3'}$ refer to the dGs in the dGGG triplet of each respective duplex. Values are the average \pm std. dev. of 3 replicates.

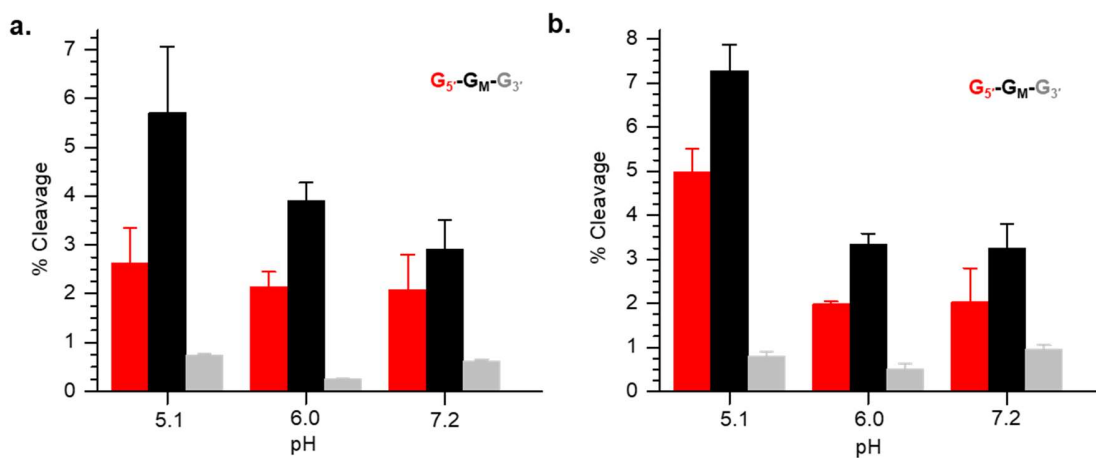


Figure S16. pH Effect on strand damage in duplex 6. (a) Fpg treatment (b) Piperidine treatment. G_5' , G_M' , and $G_{3'}$ refer to the dGs in the dGGG triplet of each respective duplex. Values are the average \pm std. dev. of 3 replicates.

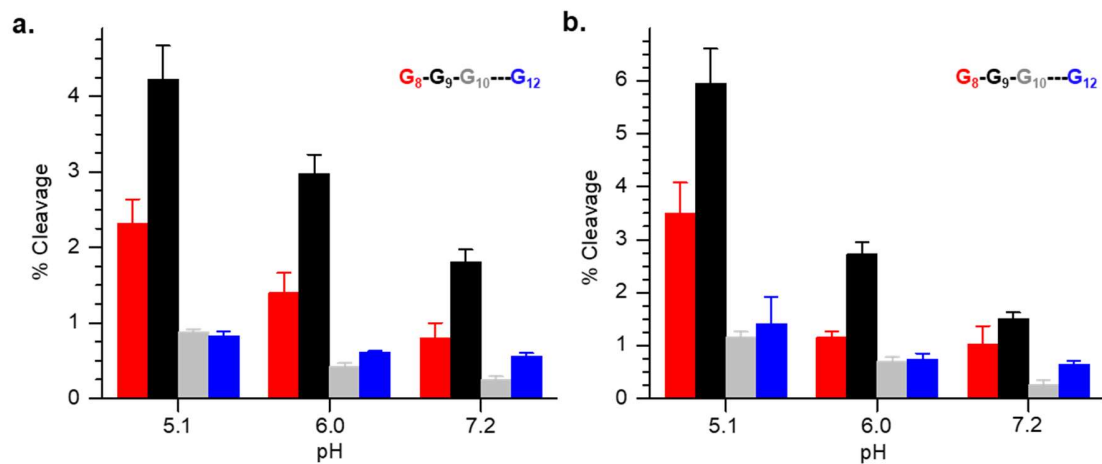


Figure S17. pH Effect on strand damage in duplex 7. (a) Fpg treatment (b) Piperidine treatment. Values are the average \pm std. dev. of 3 replicates.

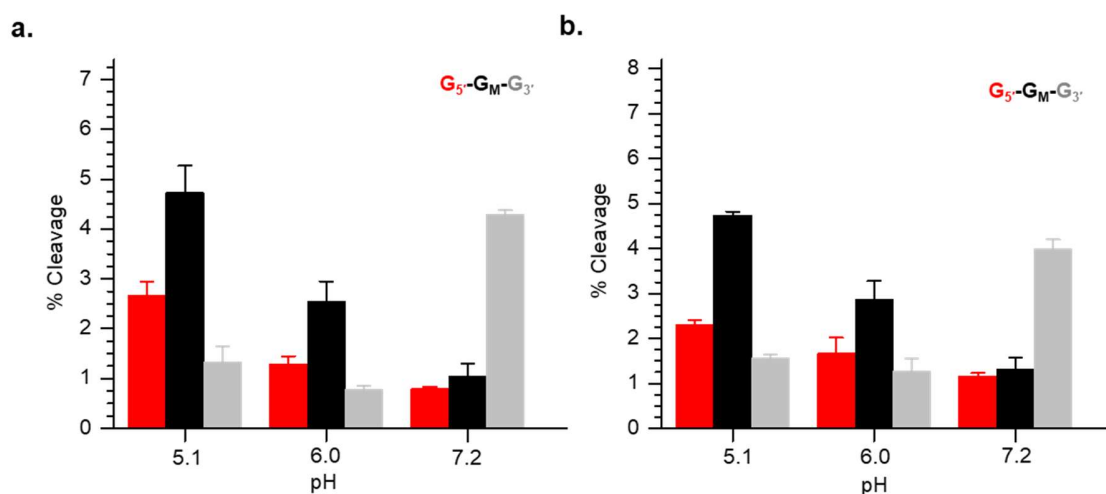


Figure S18. pH Effect on strand damage in duplex 11. (a) Fpg treatment (b) Piperidine treatment. Values are the average \pm std. dev. of 3 replicates.

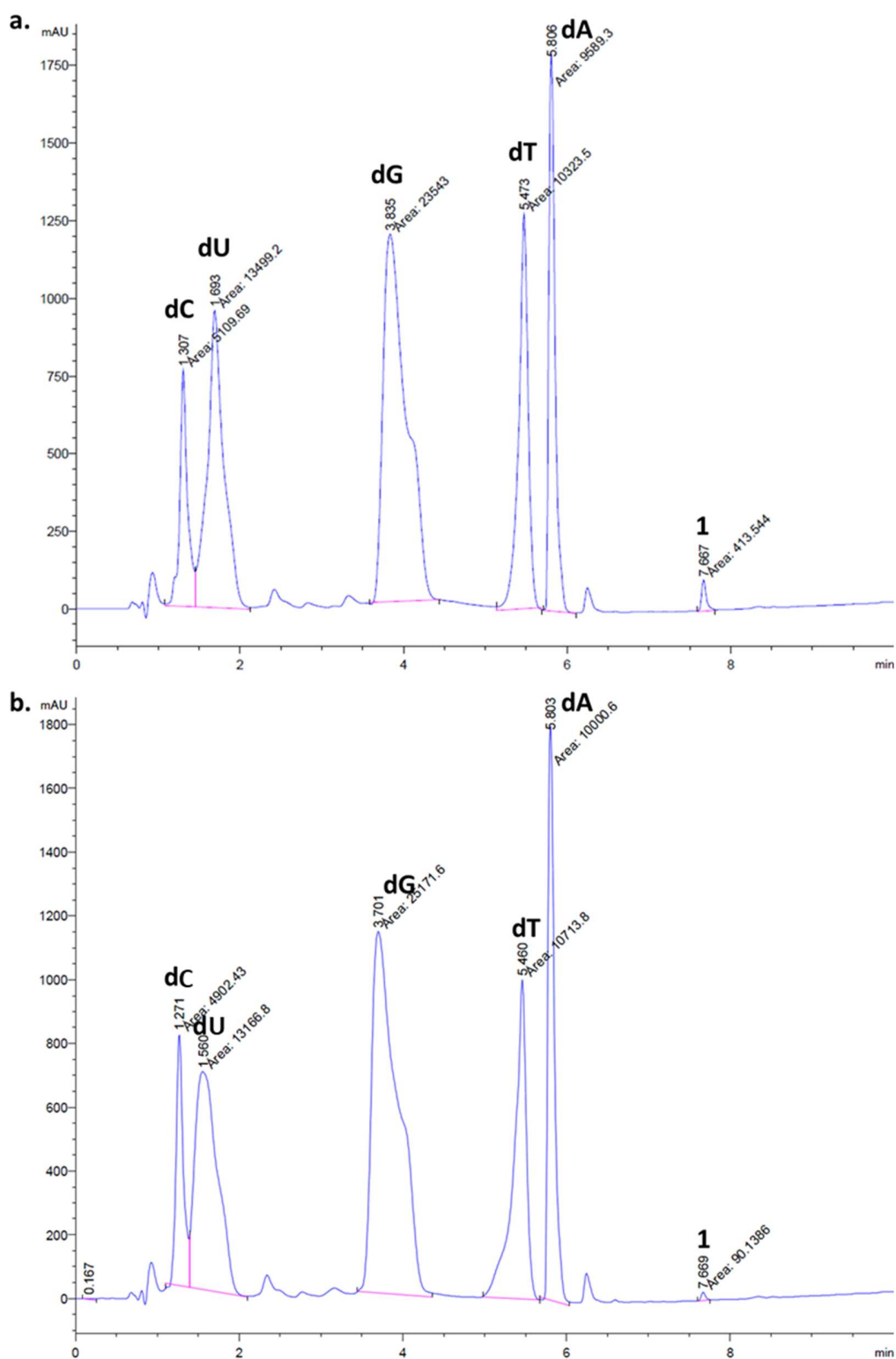


Figure S19. Chromatogram ($\lambda = 260$ nm) of a) Duplex **2** after enzyme digestion. b) Photolysate of **2** after enzyme digestion.

Table S2. Estimated efficiency of hole transfer (pH = 5.1)

Duplex	Total %cleavage on Gs	% Hole transfer ^{a,b}
6	9.06 ± 1.24	113.25 ± 15.5
7	8.1 ± 0.76	101.25 ± 9.5
8	5.83 ± 0.21	72.88 ± 2.62
9	8.67 ± 0.71	108.38 ± 8.8
10	8.03 ± 0.84	100.38 ± 10.5
11	8.64 ± 0.62	106.75 ± 5.5

a. The yield of trapping reaction of the hole is ~10%.

b. The conversion of **1** is 80% after photolysis.

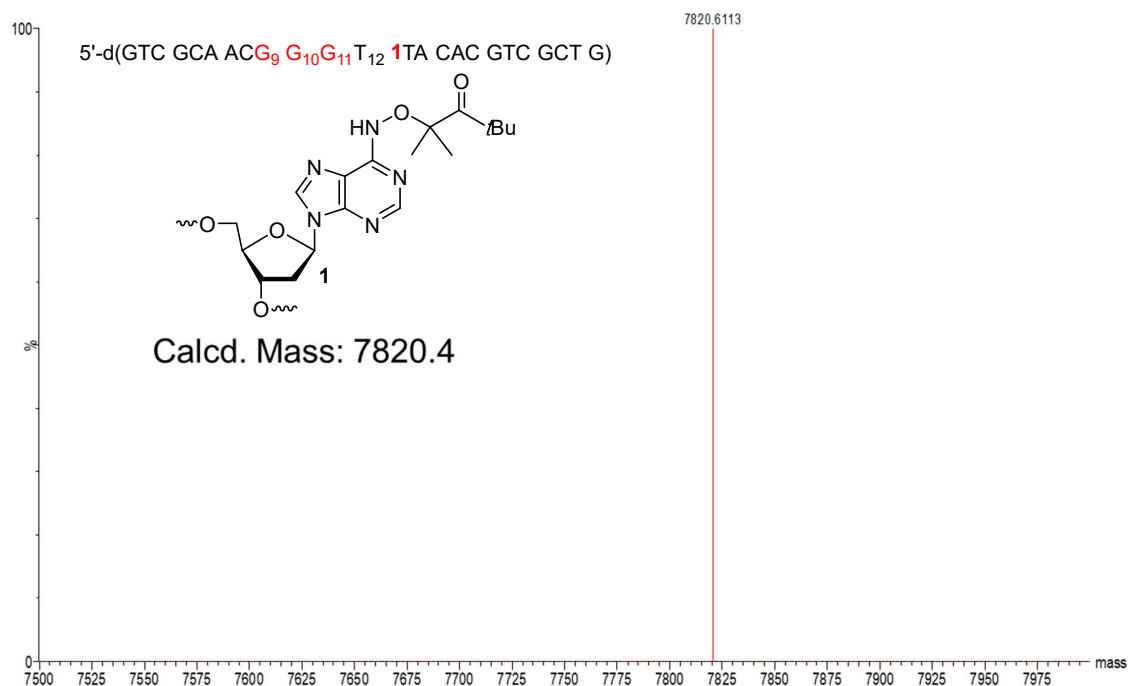


Figure S20. UPLC-MS of the strand of **2** containing **1**.

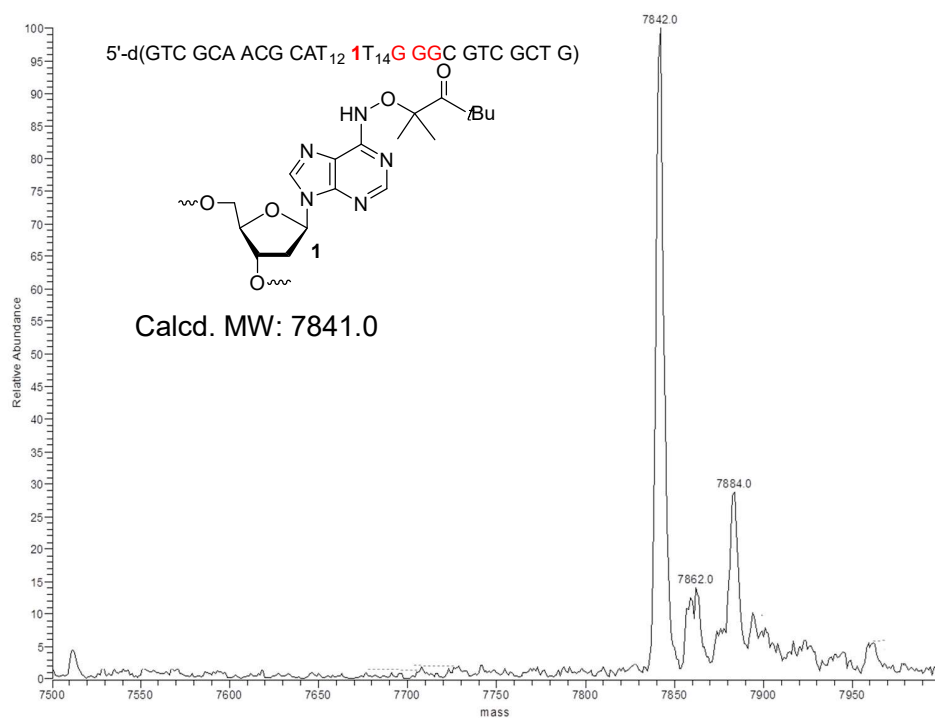


Figure S21. ESI-MS of the strand of **3** containing **1**.

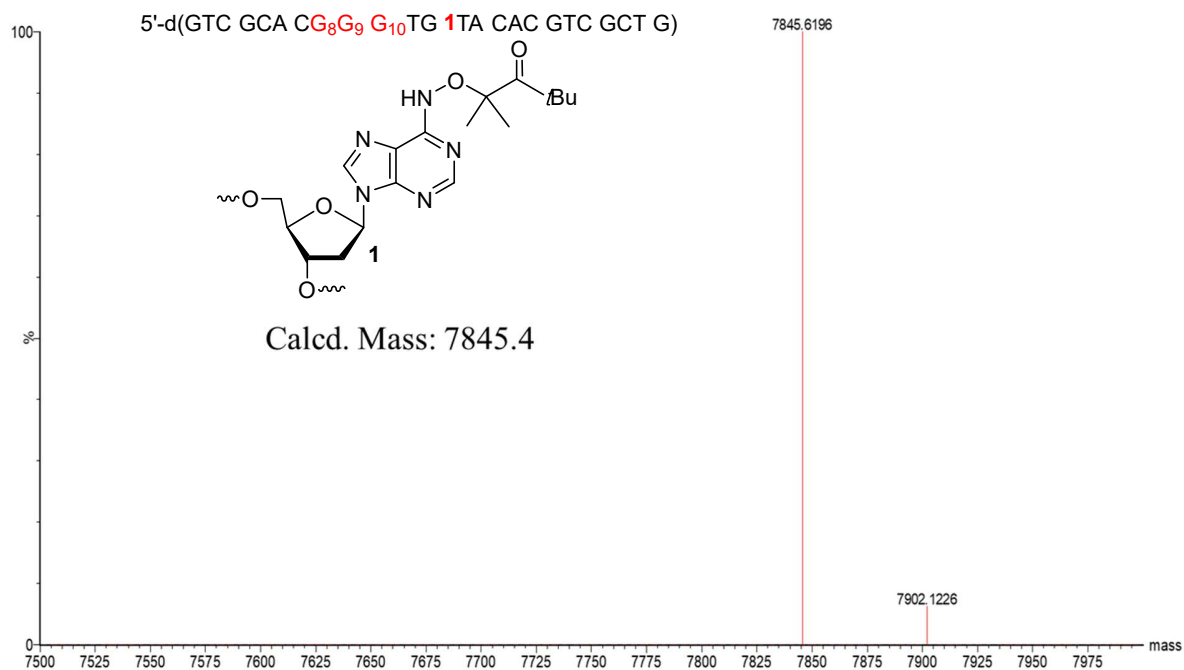


Figure S22. UPLC-MS of the strand of **4** containing **1**.

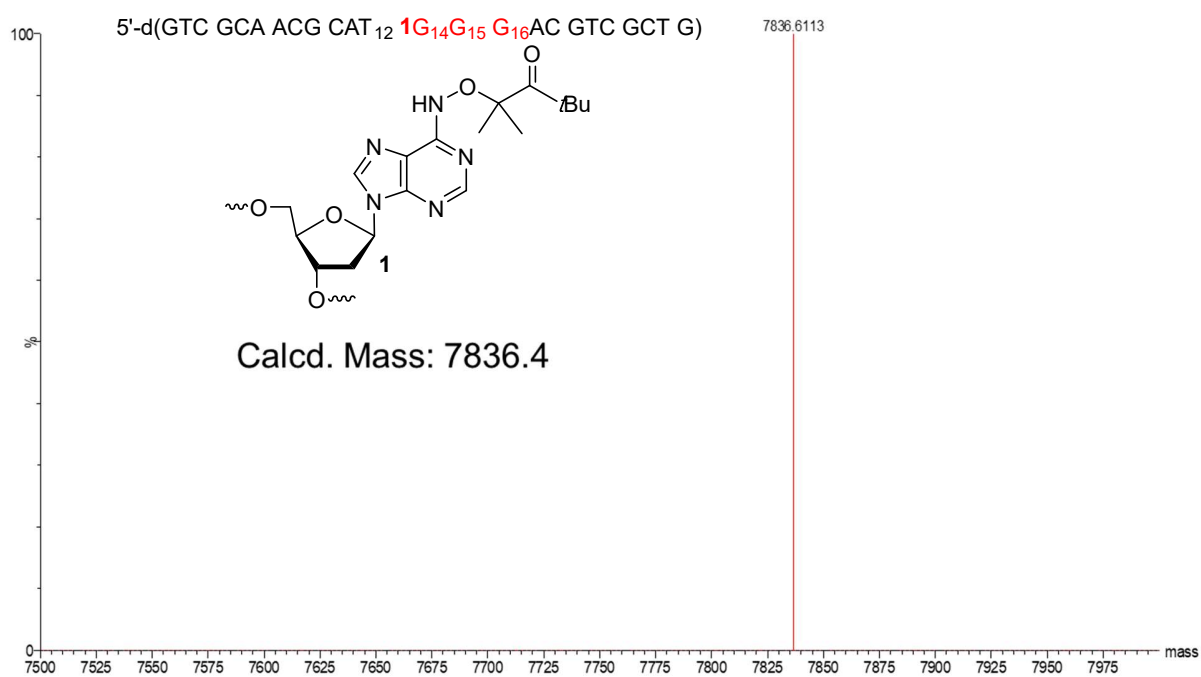


Figure S23. ESI-MS of the strand of **6** containing **1**.

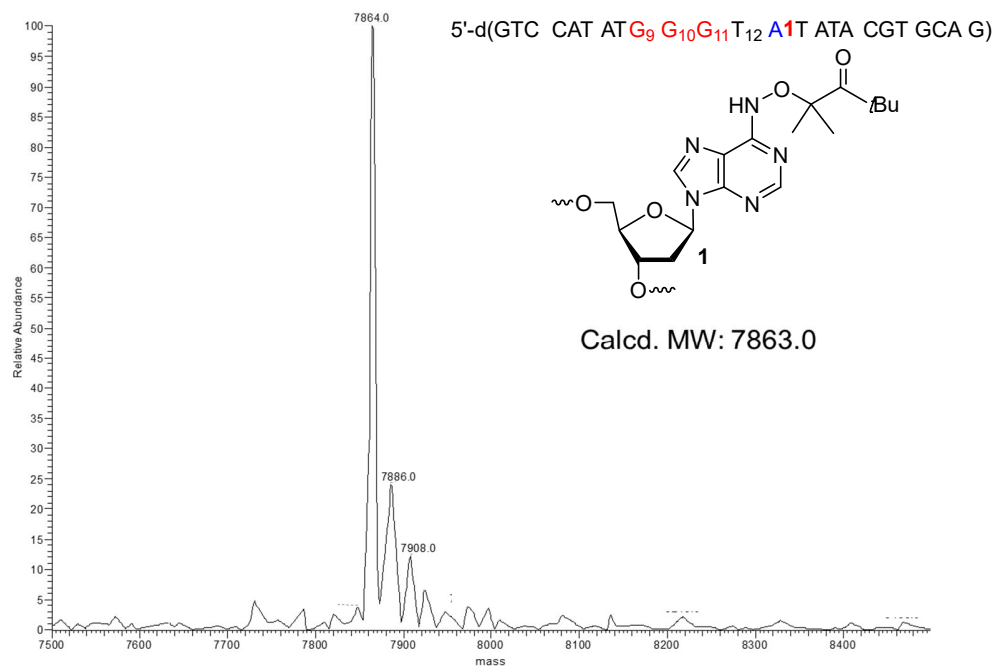


Figure S24. ESI-MS of the strand of **5** containing **1**.

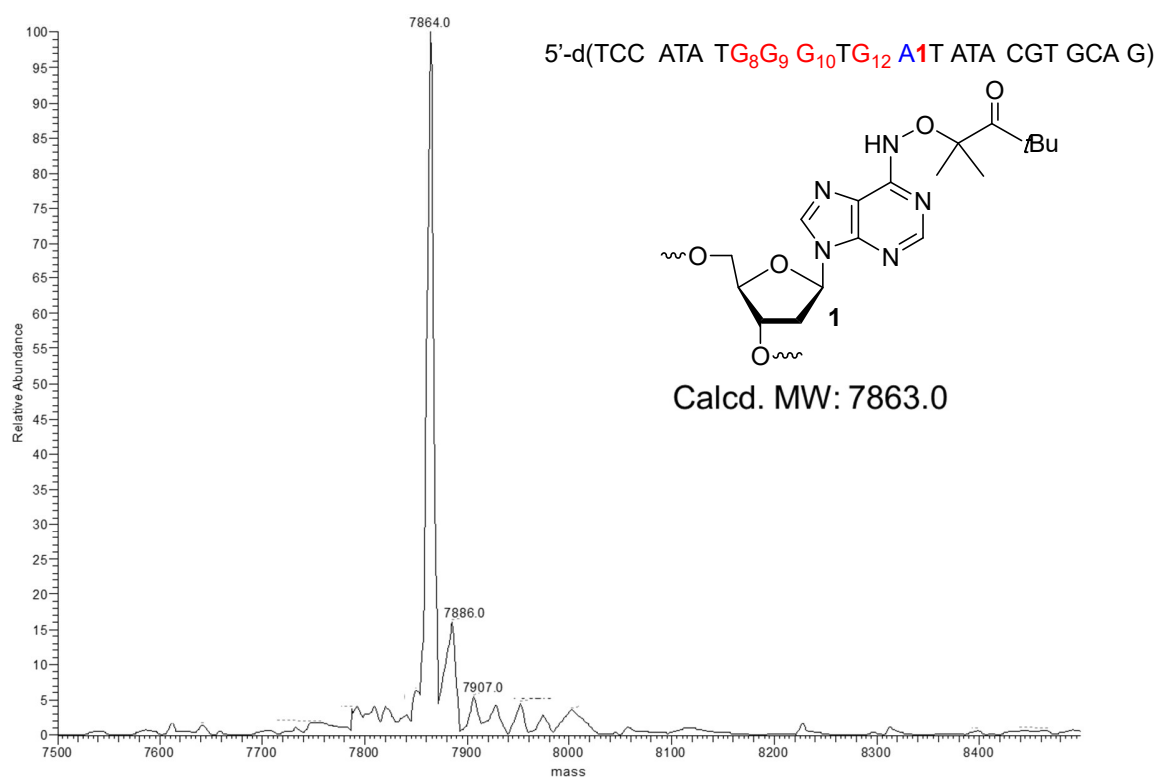


Figure S25. ESI-MS of the strand of **7** containing **1**.

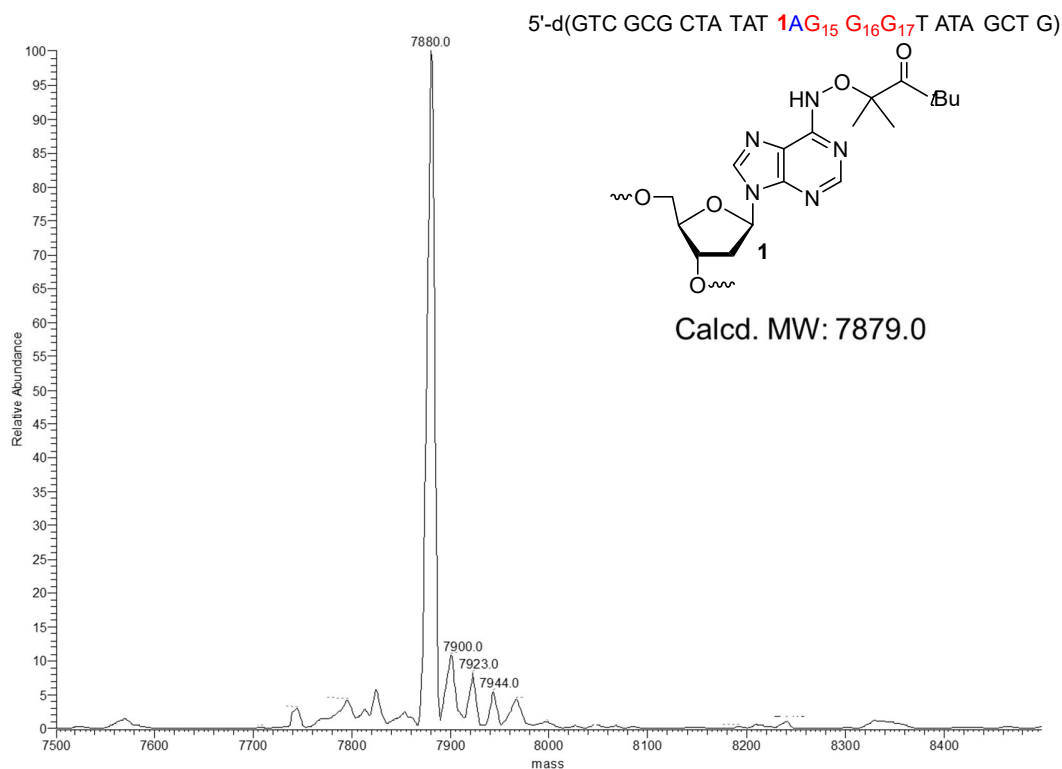


Figure S26. ESI-MS of the strand of **8** containing **1**.

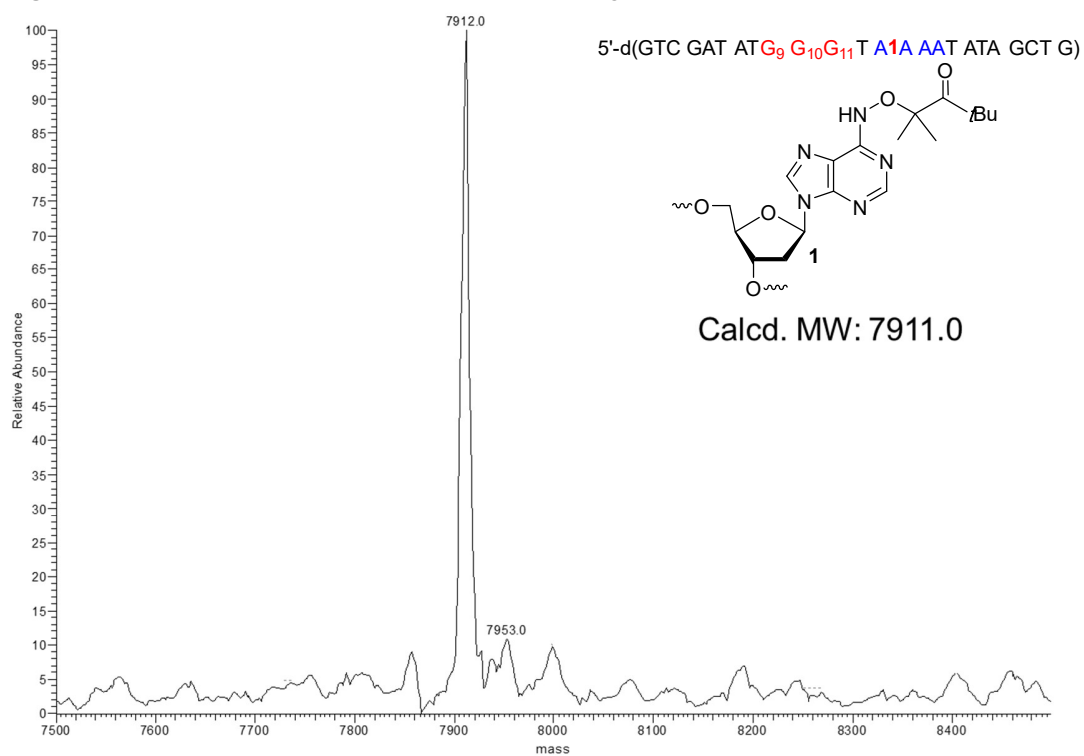


Figure S27. ESI-MS of the strand of **9** containing **1**.

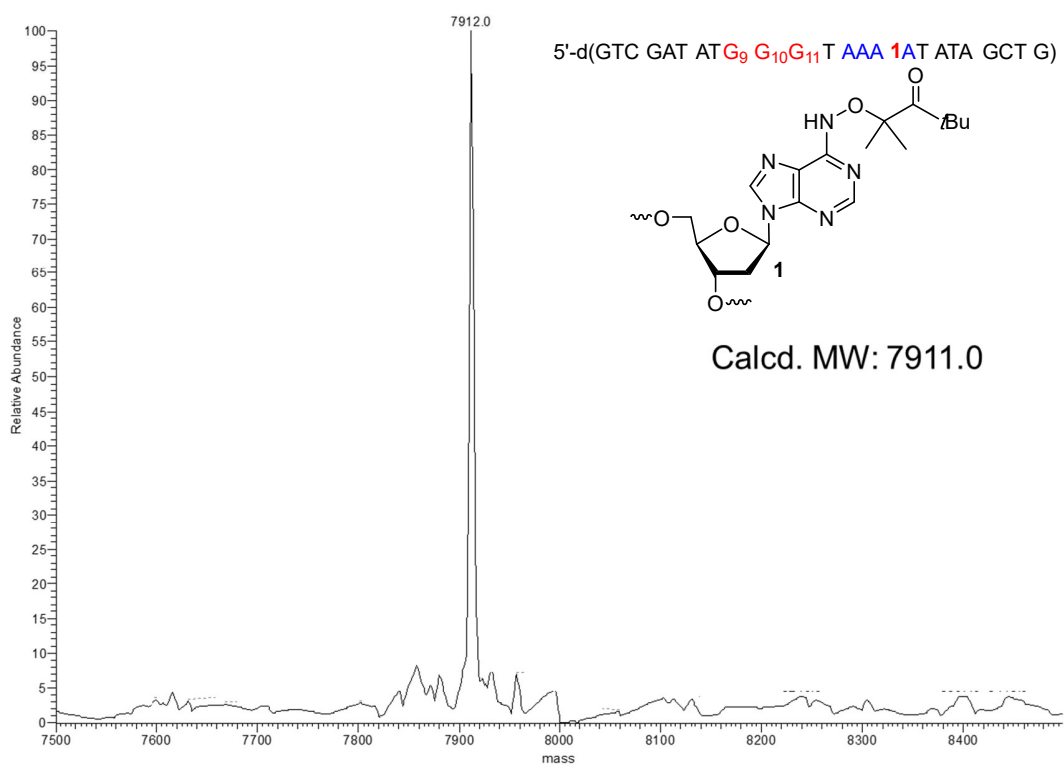


Figure S28. ESI-MS of the strand of **10** containing **1**.

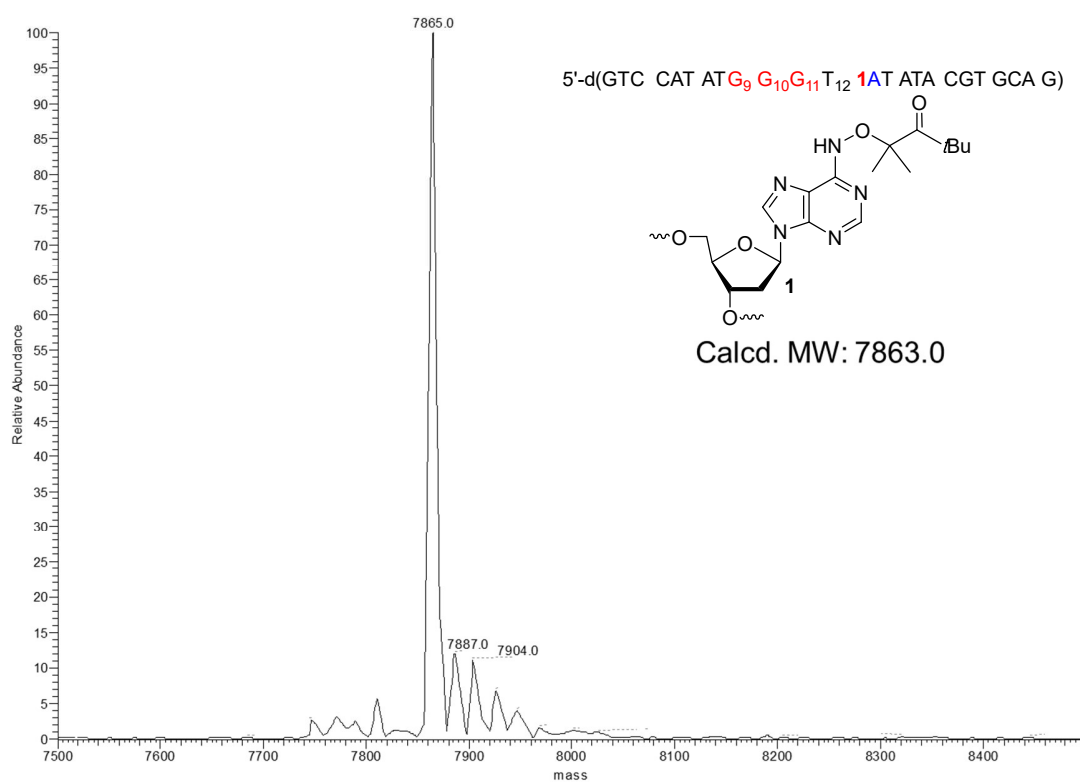


Figure S29. ESI-MS of the strand of **11** containing **1**.

